Journal of
Materials in Life Sciences

Vol. 2 No. 2 (2023)

Full Paper

Effect of Combustion Fuel on Phase, Morphology and Band Gap Energy of MgO Nanoparticles Prepared via Self-Propagating Combustion (SPC) Method

Nurhanna Badar[a,b,*], Hanis Mohd Yusoff[a,b], Intan Nur Zulayqha Nor Azmi[a], Nur Izzati Cik Mohd Marzuki[a,c], Nor Syazwanie Mohd Saidi[a] and Kelimah Elong[d,e]

[a] Faculty of Science and Marine Environment, Universiti Malaysia Terengganu, 21030 Kuala Nerus, Terengganu, Malaysia

[b] Advance Nano Materials (AnoMa) Research Group, Faculty of Science and Marine Environment, Universiti Malaysia Terengganu, 21030 Kuala Nerus, Terengganu, Malaysia

[c] Faculty of Applied Sciences, Universiti Teknologi MARA Pahang Campus, 26400 Pahang, Malaysia

[d] Centre for Functional Materials and Nanotechnology, Institute of Science, Universiti Teknologi MARA, 40450 Shah Alam, Malaysia

[e] School of Chemistry and Environment, Faculty of Applied Sciences, Universiti Teknologi MARA, 40450 Shah Alam, Malaysia

Article history
Received
14 August 2023
Revised
26 October 2023
Accepted
5 November 2023
Published online
25 November 2023

*Corresponding author
nurhanna.badar@umt.edu.my

Abstract

In this study, MgO nanoparticles (MgO-NPs) were synthesized using self-propagating combustion (SPC) method. Different fuels which are triethanolamine, glycine, and citric acid were employed to investigate their effects on the phase, morphology, particle size and band gap energy of MgO-NPs. The resulting samples were named MgO-TRI (triethanolamine), MgO-GLY (glycine), and MgO-CA (citric acid). This method is simple, produces uniform powder, and is capable of yielding large quantities of the final product. Pure MgO-NPs was obtained at the temperature of 600℃ for 12 hours. The produced nanoparticles exhibit agglomerated and irregular rounded particle size (26.43 nm) using triethanolamine as fuel followed by citric acid (51.50 nm) and glycine (90.44 nm). The band gap energy of the produced MgO-NPs ranging from 5.81 eV to 6.20 eV is much lower than their micron-sized counterpart (7.8 eV). Due to having the smallest particle size, the MgO-TRI sample has the lowest band gap energy followed by MgO-CA and MgO-GLY which have bigger particle sizes. This shows that the band gap energy of materials is affected by the size of particles. The findings indicated that the tuning of band gap energy of synthesized nanomaterials suiting the desired applications can be executed by varying the fuels. From this study, triethanolamine is evidenced to be the most effective fuel for the SPC method as it produced the smallest particle size producing MgO-NPs with the lowest band gap energy compared to other fuels.

Keywords MgO nanoparticles, self-propagating combustion, band gap, triethanolamine, citric acid, glycine

1.0 INTRODUCTION

Magnesium oxide (MgO) exhibits outstanding stability, high melting point as well as excellent resistance to chemical corrosion. Due to these unique properties, it is suitable for a wide range of physical industrial applications which include applications in catalysis, sensing, energy storage and optoelectronics [1-3]. It is also highly applicable in biological industrial applications due

to its biocompatibility and antibacterial behaviour. As stated in previous studies, MgO has been applied in biomedical and tissue engineering. It has also been applied in drug delivery [4-5]. The study of MgO has been done widely in the past. However, studies investigating the morphology, structure and optical properties need to be explored deeper. Our study focuses on investigating the characteristics of MgO nanoparticles (MgO-NPS) synthesized through the self-propagating combustion (SPC) method. The SPC method is a straightforward approach which is known to be economical. The method involves reacting metal precursors and fuels exothermically to quickly produce the desired materials. This method allows the researchers to control the morphology, particle size and particle size distribution of the materials. The production of highly crystalline nanoparticles with unique morphologies proven through the SPC method has been favoured by a lot of researchers [6-8].

This research will delve deeper into understanding the role of fuels in the SPC method as well as the effect of three different combustion fuels such as triethanolamine, glycine and citric acid on the structure, morphology and properties of the produced MgO nanoparticles. Understanding the effect of different fuels on the characteristics of MgO nanoparticles will provide us with more fuel options in the future. The results and findings will help in elucidating the relationship between the combustion synthesis parameters and the properties of MgO nanoparticles. The phase, morphology, particle size and their effects on band gap energy values will be discussed in this study. The knowledge acquired from this study can promote the development of MgO-based materials with tailored properties suiting diverse applications which will tremendously enhance the fields of catalysis, sensing, optoelectronics, energy storage and biomedical applications.

2.0 EXPERIMENTAL

2.1 Materials and Methods

In this study, the self-propagating combustion (SPC) method was employed in synthesizing the magnesium oxide nanoparticle (MgO-NPs) [9]. The SPC method involves dissolving metal precursors in deionized water, followed by the addition of fuels, initiating the combustion process at low temperatures. Three distinct fuels which are triethanolamine ($C_6H_{15}NO_3$, Merck, 99.0% purity), glycine (NH_2CH_2COOH, Sigma-Aldrich, 99.0% purity) and citric acid ($C_6H_8O_7$, Sigma-Aldrich, 99.0% purity) were utilized. The calculation of the fuel quantity needed in each synthesis for a stoichiometric balance between the precursor and fuel (φ = 1) followed the approach detailed by Jain et al. [10]. For the first experiment, 6.41 g of magnesium nitrate hexahydrate, $Mg(NO_3)_2.6H_2O$ with 99.9% purity from HmbG, was dissolved in deionized water followed by the addition of 1.13 g of triethanolamine. To ensure homogeneity, the solution was stirred for thirty minutes, and then slowly heated at 200°C until combustion occurred under ignition conditions. The resulting precursor materials were ground into fine powders using an agate mortar. This procedure was then repeated using different fuels, employing 1.59 g of citric acid and 2.08 g of glycine.

The annealing of the produced precursors was done at the temperature of 600°C for 12 hours to yield the final products, which were named MgO-TRI (triethanolamine), MgO-GLY (glycine), and MgO-CA (citric acid), respectively. XRD patterns were measured using a PanAlytical X'Pert Pro MPD instrument, with data collected at 2θ with the range of 30° to 90°. The Cu K_α radiation with λ = 1.5418 Å (40 mA and 45 kV) with Bragg-Brentano geometry was employed. The MgO-NPs samples were characterized using a Field Emission Scanning Electron Microscope (FESEM) (Model: JEOL JSM-7600F) to determine their morphology and particle size. The JSM-7600F operated with a field-emission (FE) gun for high-resolution imaging and stable gun conditions. Particle size measurements were carried out using FESEM software. The average particle size was determined by measuring approximately 50 crystals with random sizes to ensure a representative and comprehensive data collection. Additionally, reflectance spectra for the determination of the band gap energy values of the MgO-NPs samples were evaluated using a UV-visible NIR spectrophotometer (Model: Perkin-Elmer Lambda 950) with a reflection geometry. Reflectance spectra observed in the wavelength range between 190 to 300 nm were used in the band gap energies calculation using the acclaimed Tauc relation stated below:

$$(\alpha \; x \; h \; x \; v) \; = \; A \; x \; [(h \; x \; v) - \; Eg] \quad (1)$$

where α corresponds to the absorption coefficient of the material at a certain value of the wavelength λ, h refers to Planck's constant, A for a proportionality constant, v corresponds to the frequency of light and Eg represents the band energy while x=½ (for direct transition mode materials).

3.0 RESULTS AND DISCUSSION

3.1 Sample Appearance

In this study, MgO nanoparticles (MgO-NPs) were synthesized using various fuels, namely triethanolamine, glycine, and citric acid. The resulting samples were labelled as MgO-TRI, MgO-GLY, and MgO-CA, respectively. Figure 1a depicts the as-prepared MgO precursors, while Figure 1b depicts the annealed MgO samples. The observed colours of the MgO-GLY, MgO-CA, and MgO-TRI precursors are brown, white, and pale brown, respectively. Notably, after annealing, all MgO samples exhibited a uniform transformation into a white powder, indicative of the presence of a pure product, which was further confirmed by X-ray diffraction (XRD) analysis [11].

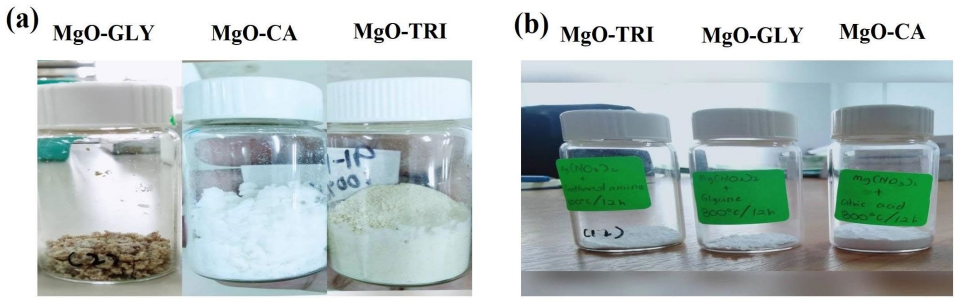

Figure 1: (a) Color appearance of the as-prepared precursors obtained for all MgO samples and (b) Color appearance of annealed materials for all MgO samples.

3.1 X-ray diffraction (XRD)

Figure 2 depicts the XRD pattern obtained for all MgO samples. The XRD patterns of MgO are compared to the MgO cubic structure (ICDD reference pattern no. 01-087-0651), which belongs to space group Fm-3m. From the results, the XRD patterns of MgO samples obtained display the diffraction peaks of (111), (200), (220), (311), and (222), which match the MgO cubic structure [12]. The results indicate that all the MgO samples are pure. There are no other peaks that might indicate impurities or other phases. This suggests that annealing the precursor at 600°C for 12 hours yields pure and single-phase materials [13]. Based on the XRD findings, it is concluded that the self-propagating combustion method utilizing triethanolamine, glycine, and citric acid enables the production of pure MgO compounds.

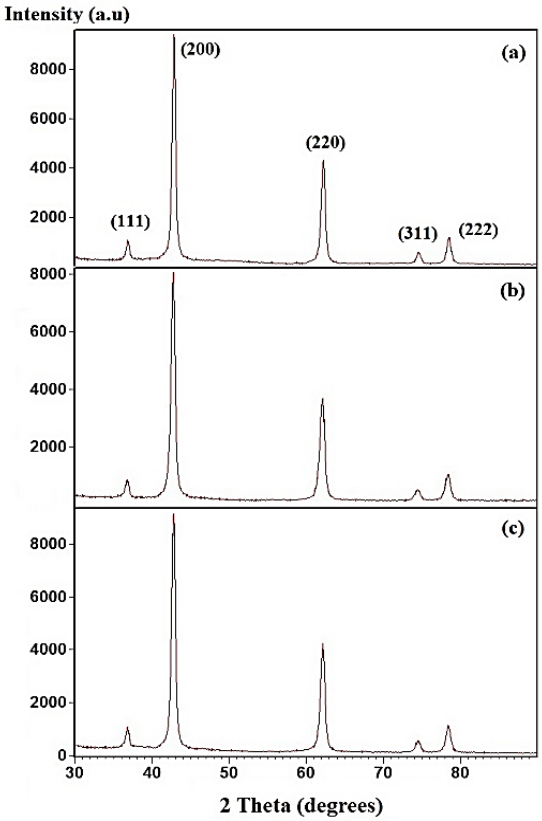

Figure 2: XRD Patterns for (a) MgO-TRI, (b) MgO-GLY and (c) MgO-CA.

3.2 Field Emission Scanning Electron Microscope (FESEM)

Morphological studies using FESEM were conducted on the MgO samples, as depicted in Figure 3. It is observed that annealing the samples at 600°C results in smaller particle sizes, less than 100 nm, regardless of the synthesis route using

triethanolamine, glycine, or citric acid. Therefore, the successful synthesis of MgO-NPs was achieved at an annealing temperature of 600°C for 12 hours. This can be attributed to the high rate of the combustion reaction, which occurs so rapidly that there isn't enough time or energy for the atoms to diffuse across large distances and the crystallites to grow significantly. Therefore, the initial nanophase is maintained [14]. The morphology of MgO-TRI, MgO-GLY and MgO-CA samples does not exhibit significant variations, indicating that the particles are made up of highly agglomerated, irregularly rounded crystals. These particles consist of small crystallites joined together by grain boundary crystallites. The observed uniformity in smaller and homogeneous grains with agglomeration is attributed to the significant release of gases during combustion [14-16].

Table 1 provides a summary of the average particle sizes measured randomly using FESEM software for various samples. The average particle sizes for MgO-TRI, MgO-GLY, and MgO-CA are approximately 26.43 nm, 90.44 nm, and 51.50 nm, respectively. The results indicate that the self-propagating combustion (SPC) route utilizing triethanolamine yields the smallest particle size, followed by citric acid and glycine. The observed discrepancy in particle size among MgO samples synthesized using distinct fuels can be explained by the different combustion characteristics and thermal effects associated with each fuel, which can influence the nucleation process and growth of particles during the synthesis. As reported by Sedghi et al. [14], the enthalpy or flame temperature during combustion can impact material characteristics, including crystallite size and agglomeration. The enthalpies of combustion ($\Delta_c H_{solid}$) for triethanolamine, glycine, and citric acid are -3840.6 ± 1.5 KJ/mol, -974.1 ± 0.5 KJ/mol, and -1906.0 ± 4.6 KJ/mol, respectively [17]. This difference in enthalpy explains the advantageous formation of smaller particles and a more porous structure when using triethanolamine, which possesses a higher enthalpy compared to others [18-19]. In summary, the selection of different fuels introduces distinct combustion dynamics, influencing the nucleation and growth of MgO crystallites. Triethanolamine, glycine, and citric acid each contribute unique combustion properties, resulting in the observed variations in average particle sizes for MgO-TRI, MgO-GLY, and MgO-CA, respectively.

MgO nanoparticles, crucial for diverse applications, display varied sizes depending on the synthesis methods. According to Todan et al. [20], hydrothermal, sol-gel, and microwave irradiation processes produce MgO nanoparticles with distinct characteristics. Hydrothermal synthesis yields tabular aggregates averaging 106 ± 38 nm with rod-like structures. Sol-gel synthesis results in duplex-shaped particles, with individual particles at 40 ± 9 nm. The average size of the nearly spherical aggregates produced by microwave irradiation is 96 ± 14 nm. In a study by Salman et al. [21], modified sol-gel synthesis produces smaller MgO nanoparticles (30-50 nm) with surface agglomeration. Additionally, Nassar et al. [15] synthesized MgO-NPs using a hybrid sol-gel combustion method with different fuels, resulting in irregular hexagonal (urea), cubic (oxalic acid), and spherical (citric acid) shaped particles with average diameters of 89 nm, 53 nm, and 81 nm, respectively. The diverse morphologies are attributed to variations in the heat and gas production during combustion, influencing crystallite sizes.

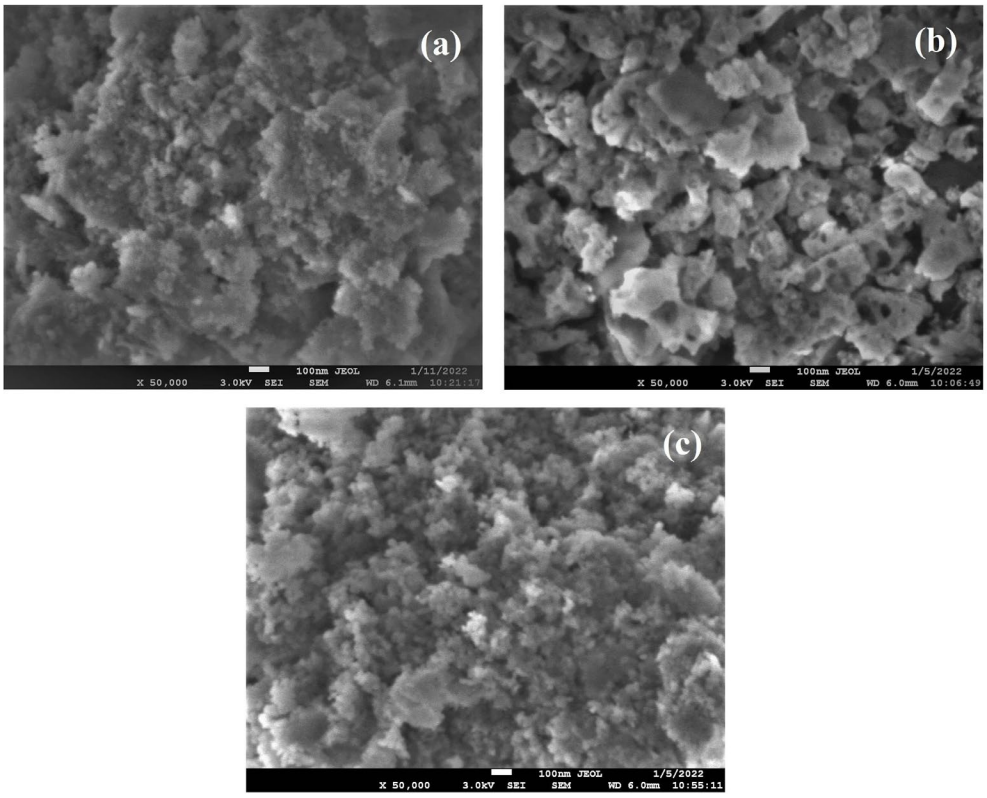

Figure 3: FESEM images of (a) MgO-TRI (b) MgO-GLY and (c) MgO-CA samples at a magnification of 50,000X.

3.3 UV-Visible NIR spectrometer with a reflection geometry

Figure 4 displays the reflectance spectra of the samples, while Figure 5 shows Tauc plots for all samples. The band gap energies that were determined using the Tauc plot are summarized in Table 1.

Table 1: Band gap energies of MgO samples.

Samples	Average particle size (nm)	Band gap energy (eV)
MgO-TRI	26.43	5.81
MgO-GLY	90.44	6.20
MgO-CA	51.50	5.90

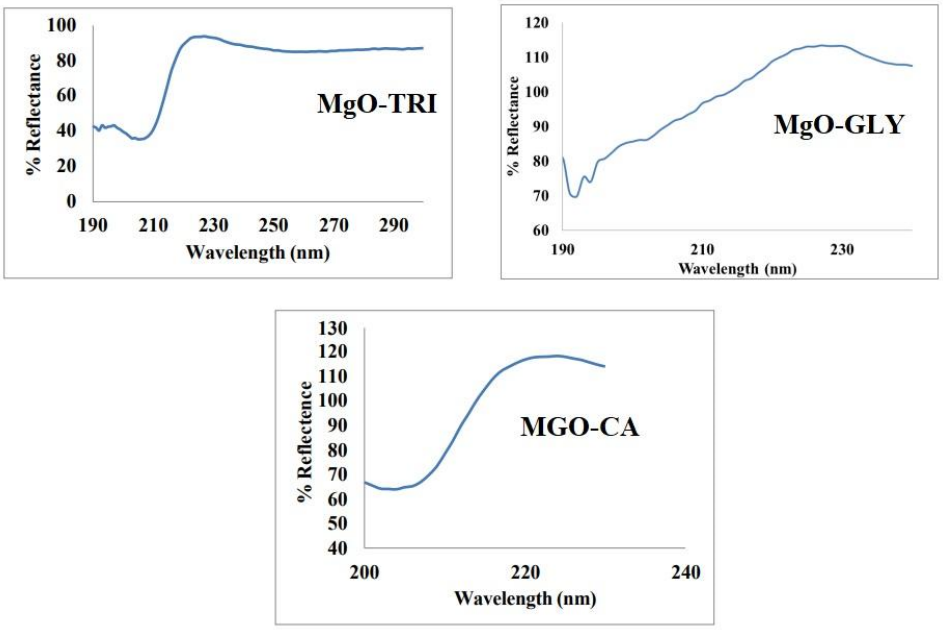

Figure 4: UV-Vis NIR spectrum for (a) MgO-TRI, (b) MgO-GLY and (c) MGO-CA samples

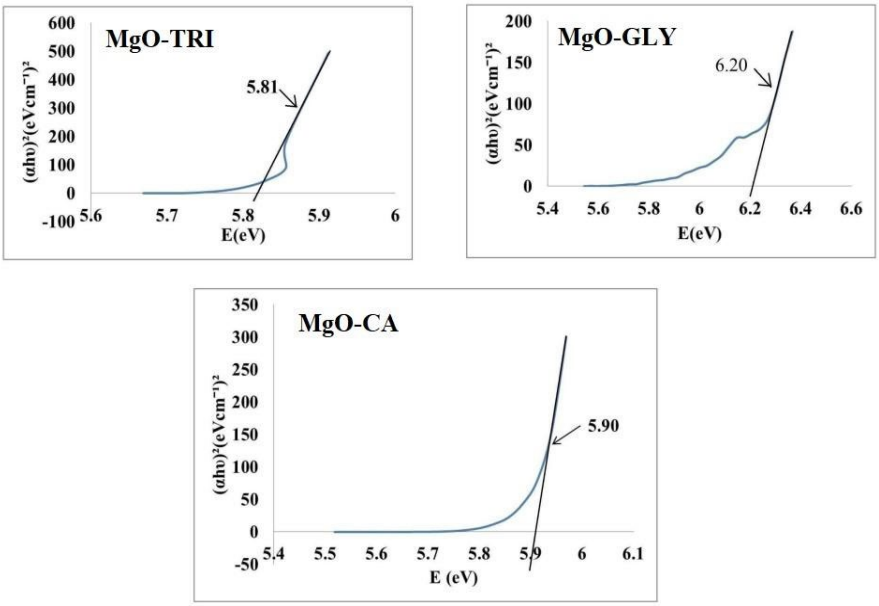

Figure 5: Tauc plot for (a) MgO-TRI, (b) MgO-GLY and (c) MGO-CA samples.

Among the samples, MgO-TRI exhibited the smallest band gap energy of 5.81 eV, while MgO-CA had a slightly higher value of 5.90 eV, and MgO-GLY had the highest band gap energy of 6.20 eV. The variance in particle sizes among the samples can be the reason for this discrepancy in band gap energies [22–23]. MgO-TRI, with its smaller particle size, demonstrates a lower band gap energy compared to MgO-CA and MgO-GLY. The observed band gap values for nano-sized MgO in this study align with the findings from Prado et al. [22] and Kumar et al. [24], where band gap energies ranging from 5.85 to 6.50 and 5.0 to 6.2 eV, respectively, were reported. Notably, the band gap energy values obtained in this study for all MgO-NPs samples are less than the band gap energy reported for its bulk counterpart by Gallagher et al. (7.8 eV) [25]. This decrease in band gap energy is due to the reduction in particle size. In the nano-region, the large surface area to volume ratio of the crystallites may lead to band gap narrowing. In summary, the findings show that the band gap energy reduces as the particle size decreases.

4.0 CONCLUSION

In summary, pure and single-phase MgO-NPs produced using different fuels which are triethanolamine, glycine and citric acid were successfully synthesized through the self-propagating combustion (SPC) method. The synthesized MgO-NPs were characterized to find out their phase, morphology, particle size and band gap energy. The optimization of combustion synthesis parameters was also done to achieve the best MgO-NPs. The band gap energy of MgO nanoparticles synthesized through the SPC method which ranges from 5.81 eV to 6.20 eV is much lower than the band gap energy of micron-sized MgO (7.8 eV). From the samples, it can be deduced that MgO-TRI have the smallest value of band gap energy of 5.81 eV followed by MgO-CA with a slightly higher value of 5.90 eV and MgO-GLY having the highest band gap energy of 6.20 eV. It was observed that the band gap energy values differ with different particle sizes of MgO-NPs produced by different fuels, indicating the importance of varying the fuel options. Furthermore, it is evidenced that the tuning of band gap energies suiting different specific applications can be executed through the selection of the appropriate fuels. All in all, the successful synthesis of pure MgO-NPs through the SPC method and the capability to tailor the band gap energy through the selection of fuels emphasize the potential of MgO-NPs for a wide range of applications.

Acknowledgement

The authors would like to thank Universiti Malaysia Terengganu for providing funding support for this project (UMT/TAPE-RG/2021/55338), Faculty of Science and Marine Environment, University Malaysia Terengganu (UMT), and the Centre for Functional Materials and Nanotechnology, Institute of Science, Universiti Teknologi MARA, Shah Alam, Malaysia, for their support in completing this work.

References

[1] Abinaya, S., Kavitha, H. P., Prakash, A., Muthukrishnaraj, A. (2021). Green synthesis of magnesium oxide nanoparticles and its applications: A review. Sustainable Chemistry and Pharmacy, 19, 100368.

[2] Elwathig, A.E., Holger, B.F. (2018). Magnesium oxide as a catalyst for the dehydrogenation of n-octane. Arabian Journal of Chemistry. 11 (7), 1154–1159.

[3] Muzammil, A., Miandad, R., Muhammad, Waqas, Gehany, F., Barakat, M.A., (2019). Remediation of wastewater using various nano-materials. Arabian Journal of Chemistry, 12 (8), 4897–4919.

[4] El-Sayyad, G.S., Mosallam, F.M., El-Batal, A.I. (2018). One-pot green synthesis of magnesium oxide nanoparticles using *Penicillium chrysogenum* melanin pigment and gamma rays with antimicrobial activity against multidrug-resistant microbes. Advanced Powder Technology. 29 (11), 2616–2625.

[5] Fazli, W., Xiang-Jun, Z., Shi-Ru, J., Bai. H., Cheng, Z. (2020). Nanocomposite hydrogels as multifunctional systems for biomedical applications: current state and perspectives. Composites Part B: Engineering, 200, 108208.

[6] Nagappa, A., Chandrappa, G. T. (2007). Mesoporous nanocrystalline magnesium oxide for environmental remediation. Microporous Mesoporous Materials, 106, 212-218.

[7] Rao, K. V., Sunandana, C. S. (2007). Structure and microstructure of combustion synthesized MgO nanoparticles and nanocrystalline MgO thin films synthesized by solution growth route. Journal of Materials Science, 43, 146-154.

[8] Kamarulzaman, N., Aziz, N. D. A., Kasim, M. F., Chayed, N. F., Subban, R. H. Y., Badar, N. (2019). Anomalies in wide band gap SnO_2 nanostructures. Journal of Solid State Chemistry, 277, 271-280.

[9] Erri, P., Nader, J., Varma, A. (2008). Controlling combustion wave propagation for transition metal/alloy/cermet foam synthesis. Advanced Materials, 20, 1243−1245.

[10] Jain, S. R., Adiga, K. C., Pai Verneker, V. R. (1981). A new approach to thermochemical calculations of condensed fuel-oxidizer mixtures. Combust Flame, 40, 71–79.

[11] Balamurugan, S., Ashika, S. A., Jainshaa, J. (2023). Influence of synthesis methods (combustion and precipitation) on the formation of nanocrystalline CeO_2, MgO, and NiO phase materials, Results in Chemistry, 5, 100941.

[12] Vijayakumar, S., Chen, J., González Sánchez, Z. I., Tungare, K., Bhori, M., Durán-Lara, Anbu, P. (2023). *Moringa oleifera* gum capped MgO nanoparticles: Synthesis, characterization, cyto- and ecotoxicity assessment. International Journal of Biological Macromolecules,233,123514.

[13] Kumari, S. V. G., Pakshirajan, K., Pugazhenthi, G. (2023). Synthesis and characterization of MgO nanostructures: A comparative study on the effect of preparation route. Materials Chemistry and Physics, 294,127036.

[14] Sedghi, A., Salehkooh, E. A., Chadorbafzade, M. (2020). Effect of fuel type on the combustion reaction behavior, phase structure and morphology of $Ni_{0.5}Co_{0.5}Fe_2O_4$ nanoparticles. Materials Science-Poland, 38(2), 341-349.

[15] Nassar, M. Y., Mohamed, T. Y., Ahmed, I. S., Samir. I. (2017). MgO nanostructure via a sol-gel combustion synthesis method using different fuels: An efficient nano-adsorbent for the removal of some anionic textile dyes. Journal of Molecular Liquids, 225, 730-740.

[16] Miranda, E.A.C., Carvajal, J.F.M., Baena, O. J. R. (2015). Effect of the Fuels Glycine, Urea and Citric Acid on Synthesis of the Ceramic Pigment $ZnCr_2O_4$ by Solution Combustion. Materials Research.18(5), 1038-1043.

[17] https://webbook.nist.gov/chemistry/

[18] Elong, K., Kasim, M.F., Azahidi A., Osman, Z. (2023). $LiNi_{0.3}Mn_{0.3}Co_{0.3}O_2$ (NMC 111) cathode material synthesize via combustion Method: Effect of combustion fuel on Structure, morphology and their electrochemical performances, Materials Today: Proceedings, https://doi.org/10.1016/j.matpr.2023.02.

[19] Zeng, J., Hai, C., Ren, X., Li, X., Shen, Y., Dong, O., Zhang, L., Sun, Y., Ma, L., Zhang, X., Dong, S., Zhou, Y. (2018). Facile triethanolamine-assisted combustion synthesized layered $LiNi_{1/3}Co_{1/3}Mn_{1/3}O_2$ cathode materials with enhanced electrochemical performance for lithium-ion batteries. Journal of Alloys and Compounds, 735, 1977-1985.

[20] Todan, L., Predoana, L., Petcu, G., Preda, S., Culita, D. C., Baran, A., Trusca, R.-D., Surdu, V.-A., Vasile, B. S., Lanculescu, A.-C. (2023). Comparative Study of MgO Nanopowders Prepared by Different Chemical Methods. Gels 2023, 9, 624.

[21] Salman, K. M., Renuka, C. G. (2023). Modified sol-gel technique for the synthesis of pure MgO and ZnO nanoparticles to study structural and optical properties for optoelectronic applications. Materials Today: Proceedings, 89, 84-89.

[22] Prado, D. C., Fernandez, I., Rodríguez-Páez, J.E. (2020). MgO nanostructures: Synthesis, characterization and tentative mechanisms of nanoparticles formation, Nano-Structures & Nano-Objects, 23,100482.

[23] Tharani, K., Christy, A. J., Sagadevan, S., Nehru, L.C. (2021). Fabrication of Magnesium oxide nanoparticles using combustion method for a biological and environmental cause. Chemical Physics Letters, 763, 138216.

[24] Kumar, A., Kumar, J. (2008). On the synthesis and optical absorption studies of nano-size magnesium oxide powder. Journal of Physics and Chemistry of Solids, 69, 2764-2772.

[25] Gallagher, M. C., Fyfield, M. S., Cowin, J.P., Joyce, S. A. (1995). Imaging insulating oxides: Scanning tunneling microscopy of ultrathin MgO films on M_0(001). Surface Science, 339, L909-L913.